



HAL
open science

Generation of a human iPSC line, INMi002-A, carrying the most prevalent USH2A variant associated with Usher syndrome type 2

Carla Sanjurjo-Soriano, Nejla Erkilic, Gael Manes, Grégor Dubois, Christian Hamel, Isabelle Meunier, Vasiliki Kalatzis

► To cite this version:

Carla Sanjurjo-Soriano, Nejla Erkilic, Gael Manes, Grégor Dubois, Christian Hamel, et al.. Generation of a human iPSC line, INMi002-A, carrying the most prevalent USH2A variant associated with Usher syndrome type 2. Stem Cell Research, 2018, 33, pp.247-250. 10.1016/j.scr.2018.11.007 . hal-02307062

HAL Id: hal-02307062

<https://hal.umontpellier.fr/hal-02307062v1>

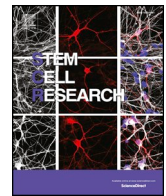
Submitted on 8 Oct 2019

HAL is a multi-disciplinary open access archive for the deposit and dissemination of scientific research documents, whether they are published or not. The documents may come from teaching and research institutions in France or abroad, or from public or private research centers.

L'archive ouverte pluridisciplinaire **HAL**, est destinée au dépôt et à la diffusion de documents scientifiques de niveau recherche, publiés ou non, émanant des établissements d'enseignement et de recherche français ou étrangers, des laboratoires publics ou privés.



Distributed under a Creative Commons Attribution 4.0 International License



Lab resource: Stem Cell Line

Generation of a human iPSC line, INMi002-A, carrying the most prevalent *USH2A* variant associated with Usher syndrome type 2



Carla Sanjurjo-Soriano^{a,b}, Nejla Erkilic^{a,b}, Gaël Manes^{a,b}, Gregor Dubois^{a,b},
Christian P. Hamel^{a,b,c}, Isabelle Meunier^{a,b,c}, Vasiliki Kalatzis^{a,b,*}

^a Inserm U1051, Institute for Neurosciences of Montpellier, Montpellier, France

^b University of Montpellier, Montpellier, France

^c Centre of Reference for Genetic Sensory Diseases, CHU, Montpellier, France

ABSTRACT

We generated an induced pluripotent stem cell (iPSC) line using dermal fibroblasts from a patient with Usher syndrome type 2 (USH2). This individual was homozygous for the most prevalent variant reported in the *USH2A* gene, c.2299delG localized in exon 13. Reprogramming was performed using the non-integrative Sendai virus reprogramming method and the human OSKM transcription factor cocktail under feeder-free culture conditions. This iPSC line will be an invaluable tool for studying the pathophysiology of USH2 and for testing the efficacy of novel treatments.

Resource table

Unique stem cell line identifier	INMi002-A
Alternative name(s) of stem cell line	<i>USH2A</i> -USH-iPSC
Institution	Institute for Neurosciences of Montpellier, Montpellier, France
Contact information of distributor	Vasiliki Kalatzis vasiliki.kalatzis@inserm.fr
Type of cell line	iPSC
Origin	Human
Additional origin info	Age: 59 years old Sex: Female Ethnicity: Caucasian
Cell Source	Dermal fibroblasts
Clonality	Clonal
Method of reprogramming	Non-integrative Sendai virus vectors
Genetic modification	Yes
Type of modification	Congenital mutation
Associated disease	Usher Syndrome type II
Gene/locus	<i>USH2A</i> , 1q41
Method of modification	N/A
Name of transgene or resistance	N/A
Inducible/constitutive system	N/A
Date archived/stock date	December 2017
Cell line repository/bank	https://hpscereg.eu/cell-line/INMi002-A
Ethical approval	Regional committee: CPP Southern Mediterranean I (2014-A00549-38) National committee: ANSM (140549B-62)

Resource utility

We established an iPSC line from a patient with Usher syndrome type 2 (USH2), characterized by retinitis pigmentosa and hearing loss, homozygous for the recurrent *USH2A* variant, c.2299delG. This line will allow modelling of the USH2 retinal and inner ear defects, and the development of novel gene and cell therapies.

Resource details

Mutations in *USH2A* cause a syndromic inherited retinal dystrophy (IRD) known as Usher syndrome type 2 (USH2), which is characterized by progressive hearing and vision loss. In addition, mutations in *USH2A* also cause a wide majority of autosomal recessive retinitis pigmentosa (RP) cases (Kremer et al., 2006). In the present study, we have generated an iPSC line from a patient with USH2 carrying a homozygous variant in exon 13 of the *USH2A* gene, c.2299delG; p.Glu767Serfs*21. This is a recurrent mutation originating from a common ancestor. Therefore, c.2299delG is observed more frequently in the population compared to the > 600 *USH2A* mutations identified (Lenassi et al., 2015), conferring a great deal of interest from a clinical perspective.

Human dermal fibroblasts were isolated and cultured from a patient skin biopsy sample and reprogrammed using an integration-free method, the CytoTune™-iPS 2.0 Sendai Reprogramming Kit. This method is based on transient overexpression of the four Yamanaka factors: *OCT3/4*, *SOX2*, *KLF4* and *c-MYC* (Takahashi et al., 2007). The morphology of the iPSC line generated displayed a typical colony

* Corresponding author at: Inserm U1051, INM, Hôpital St Eloi, BP 74103, 80 Avenue Augustin Fliche, 34091 Montpellier, France.

E-mail address: vasiliki.kalatzis@inserm.fr (V. Kalatzis).

<https://doi.org/10.1016/j.scr.2018.11.007>

Received 19 September 2018; Received in revised form 6 November 2018; Accepted 14 November 2018

Available online 16 November 2018

1873-5061/ © 2018 The Authors. Published by Elsevier B.V. This is an open access article under the CC BY license

(<http://creativecommons.org/licenses/by/4.0/>).

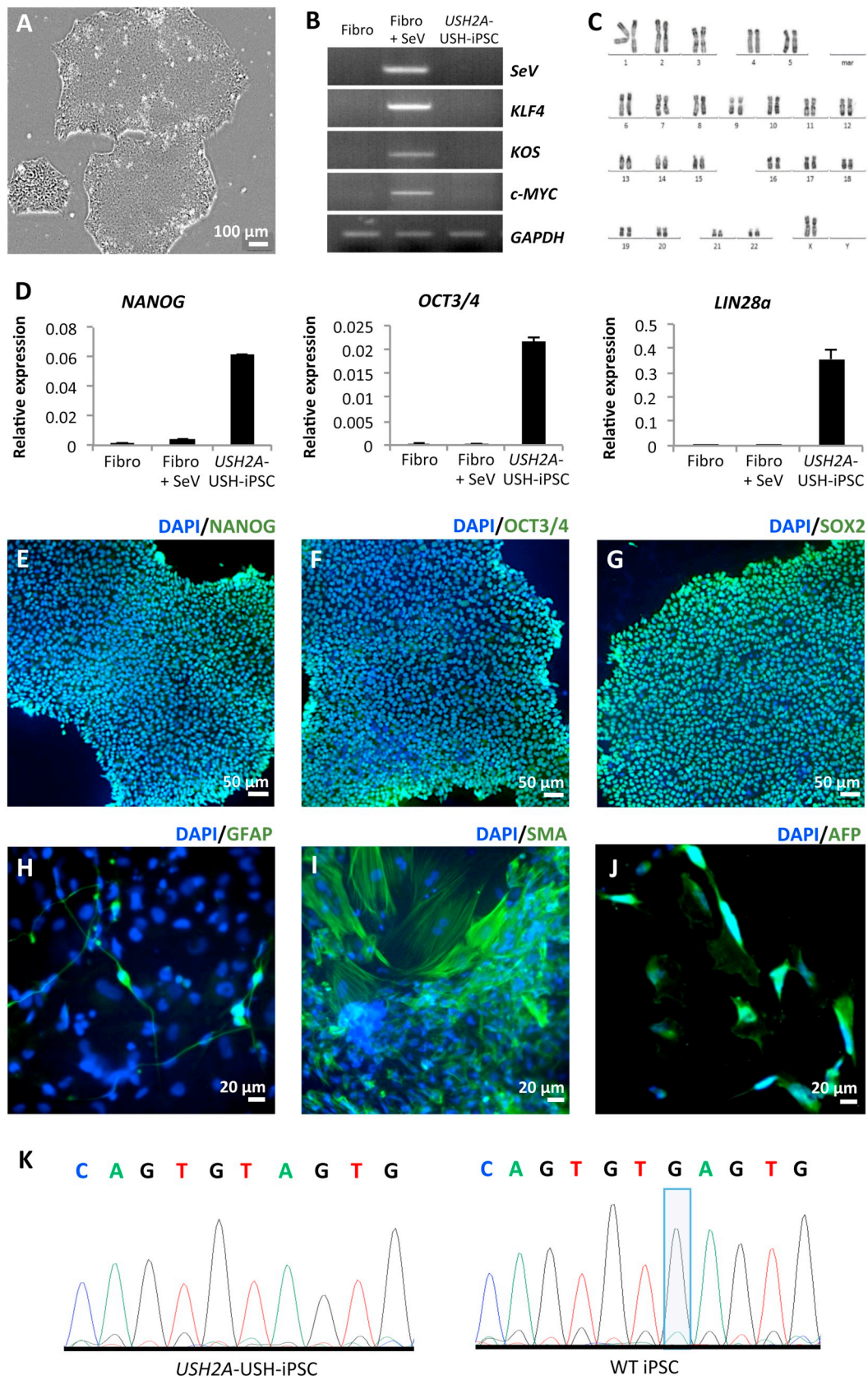


Fig. 1. Characterization of the INMi002-A (*USH2A-USH-iPSC*) line.

Table 1
Characterization and validation.

Classification	Test	Result	Data
Morphology	Photography Microscopy	Normal morphology	Fig. 1A
Phenotype	Qualitative analysis	Positive for pluripotency markers: NANOG, OCT3/4 and SOX2	Fig. 1E–1G
	Immunocytochemistry Quantitative analysis qPCR	Expression of pluripotency markers: NANOG, OCT3/4, LIN28a	Fig. 1D
Genotype Identity	Karyotype (G-banding) and resolution	46XX Resolution 400–500	Fig. 1C
	Microsatellite PCR (mPCR) OR	DNA Profiling Performed D3S306 D8S532 D11S4191 D17S787 D19S572	Available with authors
Mutation analysis	STR analysis	Not performed	N/A
	Sequencing	Homozygous, <i>USH2A</i> c.2299delG	Fig. 1K
Microbiology and virology Differentiation potential	Southern Blot OR WGS	Not performed	N/A
	Mycoplasma Embryoid body formation	Mycoplasma testing by luminescence. Negative Expression of GFAP (ectoderm), SMA (mesoderm) and AFP (endoderm) in iPSC-derived EBs	Supplementary File 1 Fig. 1H–1J
Donor screening (OPTIONAL)	Hepatitis A, Hepatitis B, Hepatitis C, HIV 1–2	Negative	Available with authors
Genotype additional info (OPTIONAL)	Blood group genotyping	N/A	N/A
	HLA tissue typing	N/A	N/A

appearance comprised of tightly packed cells (Fig. 1A). The absence of the Sendai reprogramming vectors in the INMi002-A clones was confirmed using reverse transcription (RT)-PCR. As a negative control, non-transduced patient fibroblasts (Fibro) did not carry the Sendai vectors. By contrast, the transduced fibroblasts (Fibro + SeV) expressed all three vectors that were used for reprogramming. Due to their non-integrative nature, the INMi002-A cell line had lost these vectors by passage 12 (P12) (Fig. 1B). The iPSC line generated showed a normal 46,XX karyotype at P12, which excluded major chromosomal abnormalities as a result of the reprogramming process (Fig. 1C).

Using real time polymerase chain reaction (qPCR), we showed expression of the endogenous pluripotency markers, *NANOG*, *OCT3/4* and *LIN28a* in the INMi002-A cell line when compared to non-transduced (Fibro) or transduced (Fibro + SeV; Fig. 1D) fibroblasts. The pluripotency state was further confirmed by immunofluorescence staining of NANOG (Fig. 1E), OCT3/4 (Fig. 1F) and SOX2 (Fig. 1G). The ability of the INMi002-A cell line to give rise to the three embryonic cell layers was determined by spontaneous differentiation of the iPSC into embryoid bodies (EBs). EBs were plated onto Matrigel-coated dishes and the expression of the three germ layer markers, Glial Fibrillary Acidic Protein (GFAP; ectoderm; Fig. 1H), Smooth Muscle Actin (SMA; mesoderm; Fig. 1I) and α -Fetoprotein (AFP; endoderm; Fig. 1J) was verified by immunofluorescence staining. We verified the presence of the homozygous causative mutation in exon 13 of *USH2A* (c.2299delG) in the INMi002-A iPSC, as compared to wild type iPSC, by Sanger sequencing (Fig. 1K). The identity of the patient iPSC line was confirmed by microsatellite PCR analysis in comparison to fibroblasts of the same individual and wild type iPSC (available with the authors). Lastly, the generated INMi002-A cell line was confirmed to be free of mycoplasma contamination (Supplementary File 1).

Materials and methods

Human dermal fibroblast cell culture

Dermal fibroblasts derived from a skin biopsy were cultured in AmnioMAX C100 basal media with GlutaMAX (Gibco) containing 10% decomplemented foetal calf serum (FCS; Lonza), 1% penicillin-streptomycin-amphotericin B (Lonza) and 2% AmnioMax-C100 supplement (Gibco).

iPSC generation

Fibroblasts were seeded and reprogrammed using the integration-free CytoTune™-iPS 2.0 Sendai Reprogramming Kit as previously described (Torriano et al., 2017). iPSC colonies were cultured in Essential 8 (E8) medium (Gibco) under 5% CO₂ at 37 °C, and passaged (1:10 dilution; twice weekly) using Versene (Gibco).

Karyotype analysis

Preparation of the iPSC for karyotype analysis was performed as previously described without modification (Torriano et al., 2017). Twenty metaphase spreads were counted and analyses were performed using standard G-banding procedures by the Chromostem facility (CHU Montpellier, France).

RT-PCR and qPCR analysis

RNA was extracted using the RNeasy Mini Kit (QIAGEN) and cDNA synthesis performed using the SuperScript® III First-Strand Synthesis System (Life Technologies) and random hexamers (Life Technologies), according to the manufacturer's protocols. RT-PCR was performed using a standard protocol on an Applied Biosystems Veriti 96-well thermal cycler. qPCR analysis was performed using the FastStart SYBR Green I Master mix on a LightCycler 480 II thermal cycler (Roche). Gene expression was normalized to *GAPDH*; see Table 2 for all primers.

Immunofluorescence staining

Cells were fixed using 4% PFA (20 min, RT), permeabilized with 0.1% Triton X-100 (Sigma-Aldrich; 15 min, RT) and blocked (45 min, RT) in 1% BSA (Sigma-Aldrich)/10% donkey serum (Millipore). Primary antibodies were incubated overnight, 4 °C (no primary antibody for negative control), and fluorescence-conjugated secondary antibodies 1 h, RT (Jackson ImmunoResearch). Nuclei were stained with 0.2 μ g/ml bisBenzimide (Sigma-Aldrich). Cells were observed using a Zeiss ApoTome 2 Upright wide-field microscope.

In vitro differentiation assay

iPSC were dissociated with Accutase (Stemcell Technologies) and seeded on ultra-low attachment dishes for 2 days in E8 containing

Table 2
Reagents details.

Antibodies used for immunocytochemistry/flow-cytometry			
	Antibody	Dilution	Company Cat # and RRID
Pluripotency markers	Rabbit anti-SOX2	1/200	Thermo Fisher Scientific Cat# 48–1400, RRID:AB_2533841
Pluripotency markers	Rabbit anti-NANOG	1/200	Abcam Cat# ab21624, RRID:AB_446437
Pluripotency markers	Mouse anti-OCT3/4	1/200	Santa Cruz Biotechnology Cat# sc-5279, RRID:AB_628051
Differentiation markers	Rabbit anti-GFAP	1/200	Dako Cat# Z0334, RRID:AB_10013382
Differentiation markers	Mouse anti-SMA	1/200	Dako Cat# M0851, RRID:AB_2223500
Differentiation markers	Mouse anti-AFP	1/200	Sigma Aldrich Cat# WH0000174M1, RRID:AB_1839587
Secondary antibodies	Alexa Fluor® 488 AffiniPure Donkey Anti-Rabbit IgG (H + L)	1/500	Jackson ImmunoResearch, Cat# 711-545-152, RRID:AB_2313584
Secondary antibodies	Alexa Fluor® 488 AffiniPure Donkey Anti-Mouse IgG (H + L)	1/500	Jackson ImmunoResearch, Cat# 715-545-150, RRID:AB_2340846

Primers			
	Target	Forward/Reverse primer (5'-3')	Product size (bp)
Exogenous reprogramming transgene (RT-PCR)	<i>SeV</i>	GGATCACTAGGTGATATCGAGC ACCAGACAAGAGTTTAAGAGATATGTATC	181
Exogenous reprogramming transgene (RT-PCR)	<i>KOS</i>	ATGCACCGCTACGACGTGAGCGC ACCTTGACAATCCTGATGTGG	528
Exogenous reprogramming transgene (RT-PCR)	<i>KLF4</i>	TTCTGTCATGCCAGAGGAGGCC AATGTATCGAAGGTGCTCAA	410
Exogenous reprogramming transgene (RT-PCR)	<i>c-MYC</i>	TAACTGACTAGCAGGCTTGTCG TCCACATACAGTCTGGATGATGATG	532
Pluripotency marker (RT-qPCR)	<i>NANOG</i>	CAAAAGCAAACAACCCACTT TCTGCTGGAGGCTGAGGTAT	158
Pluripotency marker (RT-qPCR)	<i>OCT3/4</i>	GTAATCCTCGGTCCTTTCC CAAAAACCCCTGGCACAACCT	168
Pluripotency marker (RT-qPCR)	<i>LIN28a</i>	GGGGAATCACCCCTACAACCT CTTGCTCCATGAATCTGGT	166
GAPDH RT-(qPCR and RT-PCR)	<i>GAPDH</i>	AACCATGAGAAGTATGACAAC CTTCCACGATACCAAAGTT	112
<i>USH2A</i> exon 13	<i>USH2A</i>	GAAGTTCATCGCAAACAGTTG CACTGATTACAGCGAAGACTG	686

Y27632 StemMACS. At day 3, the medium was changed to DMEM/F12 (Gibco) supplemented with 20% Knockout serum replacement (Gibco), 1% penicillin-streptomycin (Gibco), 1% GlutaMax (Gibco), 1% NEAA (Gibco) and 55 mM β-mercaptoethanol (Gibco). At day 7, embryoid bodies were seeded onto Matrigel-coated wells and cultured in the same medium for a further 10 days before staining.

Mutation analysis

Genomic DNA was isolated using the DNeasy Blood & Tissue Kit (Qiagen) and PCR-amplified using *USH2A*-specific primers (Table 2). The dNTPs were removed using the ExoSAP-IT PCR Clean-up kit (GE Healthcare) and the amplicon sequenced using the BigDye Terminator Cycle Sequencing Ready Reaction kit V3.1 on an Applied Biosystems 3130xL Genetic Analyzer.

Microsatellite PCR analysis

Genomic DNA was amplified using primers for informative markers (Table 1). The PCR products were mixed with Genescan 400HD ROX size standard and subsequently analyzed on an Applied Biosystems 3130xL genetic analyzer.

Mycoplasma analysis

Mycoplasma detection was performed on cell culture supernatant using the MycoAlert Mycoplasma Detection Kit (Lonza), according to the manufacturer's instructions, and a CLARIOstar microplate reader (BMG Labtech).

Acknowledgements

The authors are grateful to the patient who contributed to this study. We thank Audrey Senechal (Neurogenetic facility, INM, Montpellier) for help with sequencing analysis, Pauline Bouret and Franck Pellestor (Chromostem facility, CHU Montpellier) for karyotype analyses, and Daria Mamaeva and Stephanie Venteo (INM) for helpful discussions. This work was supported by Aviesan-Unadev, Vaincre Usher 2 and SOS retinite.

Appendix A. Supplementary data

Supplementary data to this article can be found online at <https://doi.org/10.1016/j.scr.2018.11.007>.

References

- Kremer, H., van Wijk, E., Marker, T., Wolfrum, U., Roepman, R., 2006. Usher syndrome: molecular links of pathogenesis, proteins and pathways. *Hum. Mol. Genet.* 15 (2), 262–270. <https://doi.org/10.1093/hmg/ddl205>.
- Lenassi, E., Vincent, A., Li, Z., Saihan, Z., Coffey, A.J., Steele-Stallard, H.B., ... Webster, A.R., 2015. A detailed clinical and molecular survey of subjects with nonsyndromic *USH2A* retinopathy reveals an allelic hierarchy of disease-causing variants. *Eur. J. Hum. Genet.* 23 (10), 1318–1327. <https://doi.org/10.1038/ejhg.2014.283>.
- Takahashi, K., Tanabe, K., Ohnuki, M., Narita, M., Ichisaka, T., Tomoda, K., Yamanaka, S., 2007. Induction of pluripotent stem cells from adult human fibroblasts by defined factors. *Cell* 131 (5), 861–872. <https://doi.org/10.1016/j.cell.2007.11.019>.
- Torriano, S., Erkilic, N., Faugère, V., Damodar, K., Hamel, C.P., Roux, A.-F., Kalatzis, V., 2017. Pathogenicity of a novel missense variant associated with choroideremia and its impact on gene replacement therapy. *Hum. Mol. Genet.* 26 (18), 3573–3584. <https://doi.org/10.1093/hmg/ddx244>.